Supplementary Figure 1

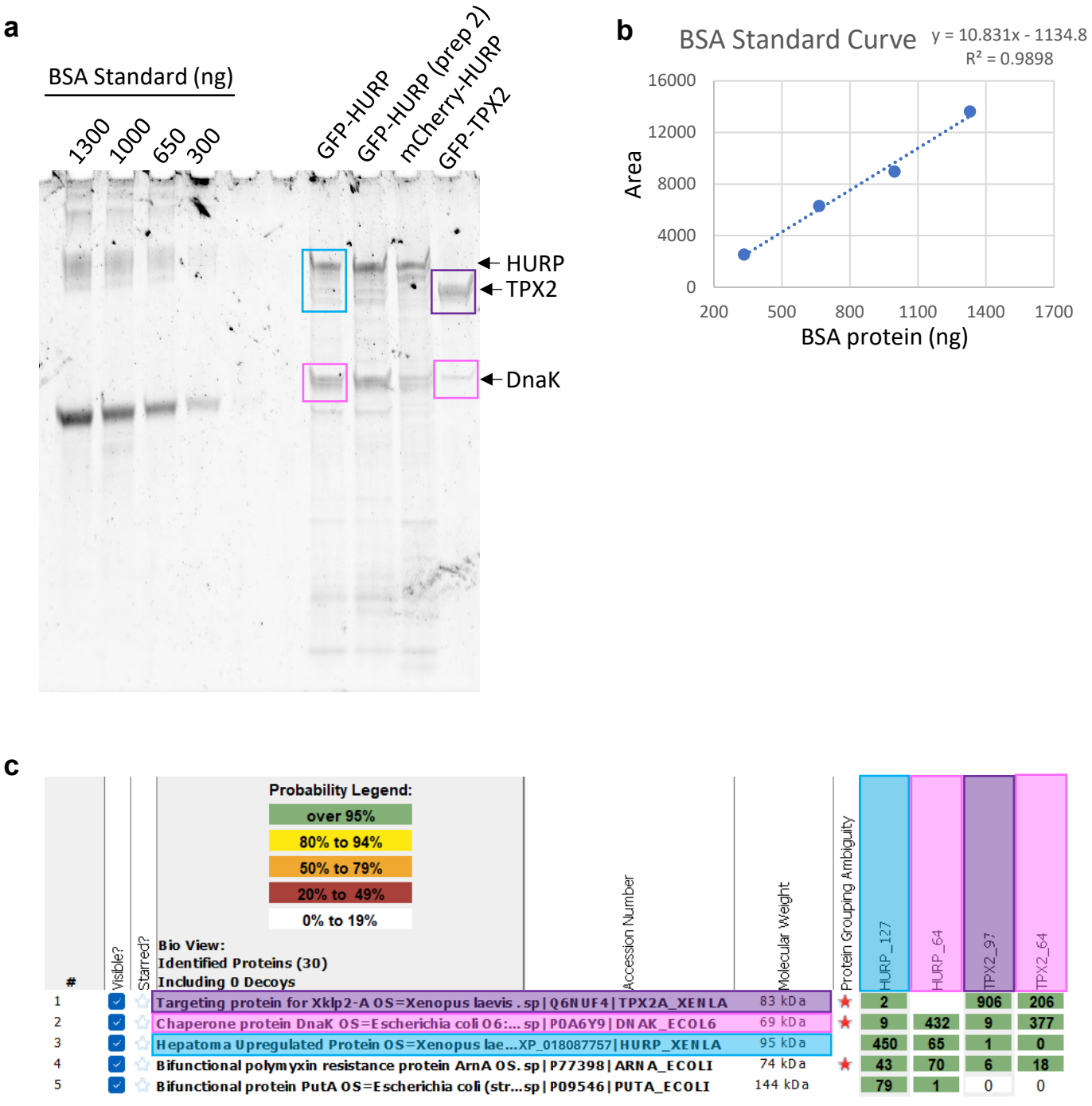

Supplementary Figure 1: Analysis of purified recombinant proteins

a SyproRuby stained gel of purified recombinant proteins with a BSA standard used for quantification of the full-length recombinant proteins. Gel bands that were excised and sent for mass spectrometry analysis (panel c) are boxed. The identity of the protein bands identified are denoted on the right of the gel. The uncropped gel is available in the source data file. **b** Standard curve of the BSA standards in panel a. **c** Analysis using Scaffold5 software[1] of LC-MS/MS data from the bands denoted in panel (color matched). The top five identified proteins, ranked by total peptide count, are shown. Numbers boxed in green denote total peptide counts.

Supplementary Figure 2

a

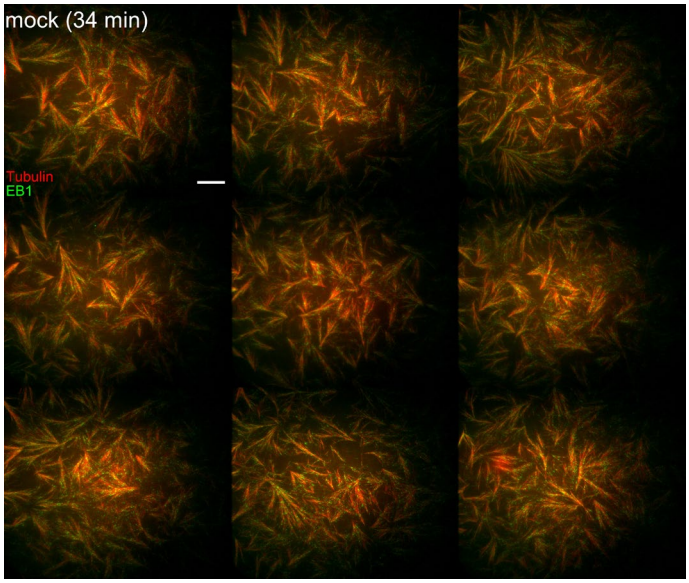

b

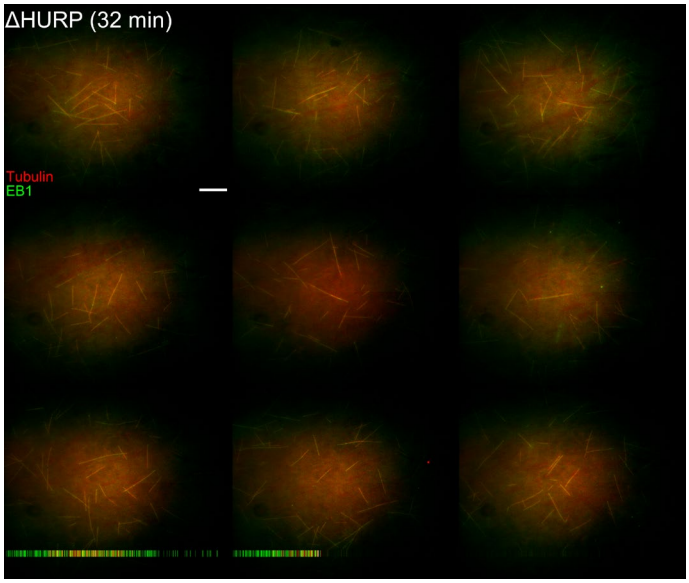

c

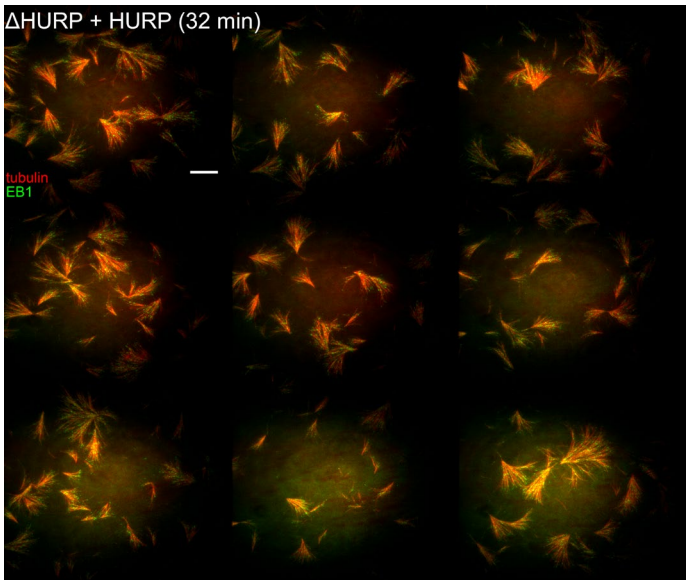

Supplementary Figure 2: HURP is necessary for branching microtubule nucleation in *Xenopus* egg extract

3 x 3 images taken of the branching microtubule (MT) nucleation reactions after obtaining the movies displayed in Supplementary Movie 1. This was done to ensure that each movie obtained was representative of the reaction. **a** 3 x 3 image of the mock depletion condition after 34 minutes. **b** 3 x 3 image of HURP-depleted condition after 32 minutes. **c** 3 x 3 image of the HURP-depleted + 250 nM purified HURP condition after 32 minutes. MTs (Alexa647-tubulin) are pseudo-colored red and EB1-mCherry is pseudo-colored green for display purposes. Total field of view is 491.55 µm x 414.75 µm. Scale bars = 20µm.

Supplementary Figure 3

Mock (30 branched structures)

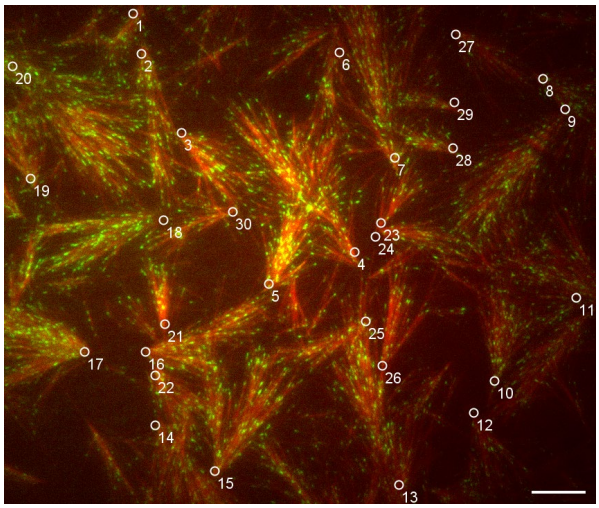

ΔHURP + HURP (9 branched structures)

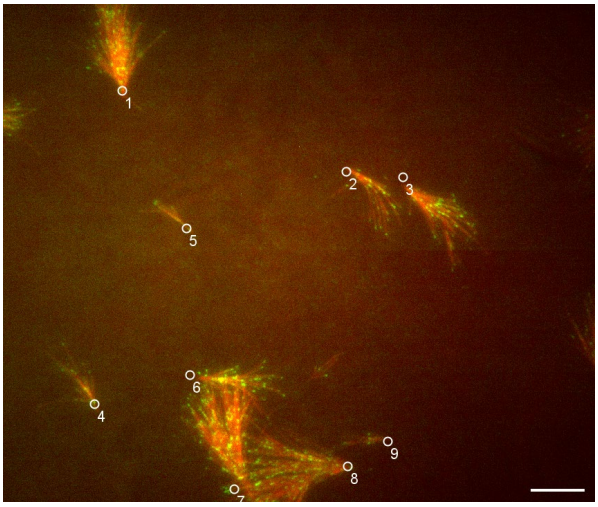

Supplementary Figure 3: Example quantification of branched structures in mock-depleted and ΔHURP + HURP *Xenopus* egg extract

Representative 110.03 µm x 92.77 µm cropped images used for obtaining the number of microtubules (MTs) over time (EB1 foci per frame) in Supplementary Movie 1 are displayed for the mock and ΔHURP + 250 nM HURP conditions at a timepoint of ~25 minutes. This timepoint was chosen because individual structures could still be discerned by eye. Individual structures in each condition are denoted with circles and numbered (mock = 30 structures; ΔHURP + HURP = 9 structures). The number of fans was used to normalize the number of MTs over time (EB1 foci per frame) for Fig. 1c. ΔHURP depleted extract was not included because no branched structures were formed (See Supplementary F. MTs (Alexa647-tubulin) are pseudo-colored red and EB1-mCherry is pseudo-colored green for display purposes. Scale bars = 10 µm.

Supplementary Figure 4

a

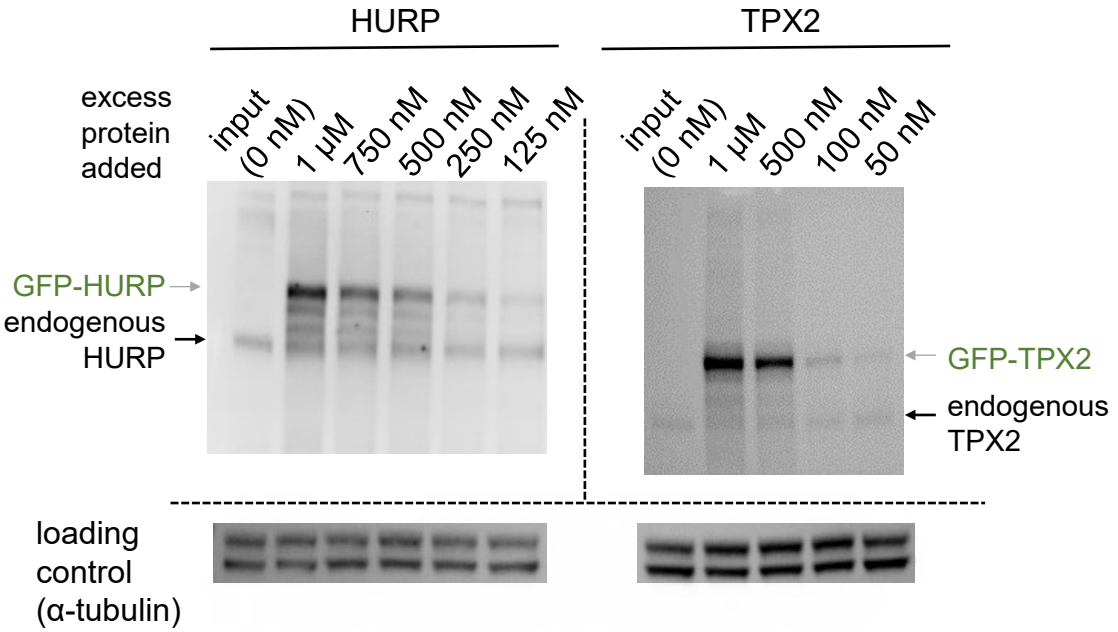

b

Concentration of excess HURP added (nM)	Expected fold increase over endogenous concentration (320 nM)[2]	Actual calculated fold increase
0	1 (input)	1 (input)
1000	4.13	5.40
750	3.34	3.69
500	2.56	2.96
250	1.78	1.59
125	1.39	1.45

Concentration of excess TPX2 added (nM)	Expected fold increase over endogenous concentration (50 nM)[2]	Actual calculated fold increase
0	1 (input)	1 (input)
1000	21	23.15
500	11	13.73
100	3	2.73
50	2	1.73

Supplementary Figure 4: Western blot assessment of fold-increase after addition of purified protein to *Xenopus laevis* egg extract

a Western blot probing for HURP and TPX2 after addition of purified recombinant proteins (GFP-tagged TPX2 and HURP) to extract. Uncropped blots are available in the source data file. **b** Densitometry analysis of the western blot, denoting expected and actual fold-increase of protein in the extract.

Supplementary Figure 5

a

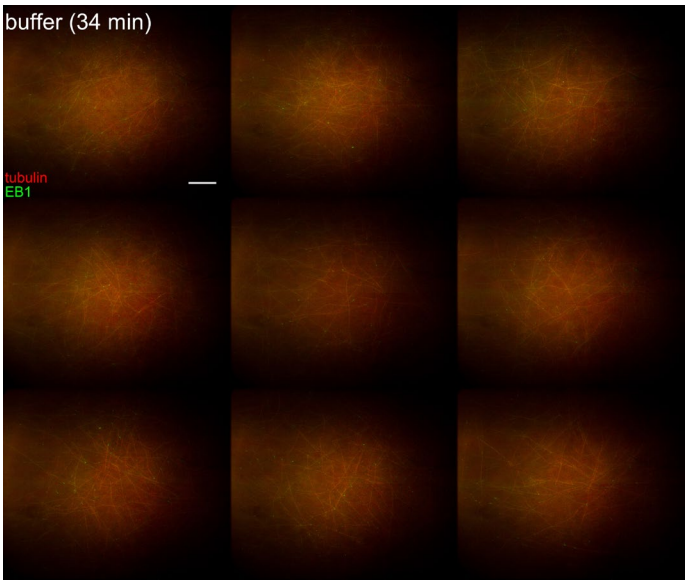

b

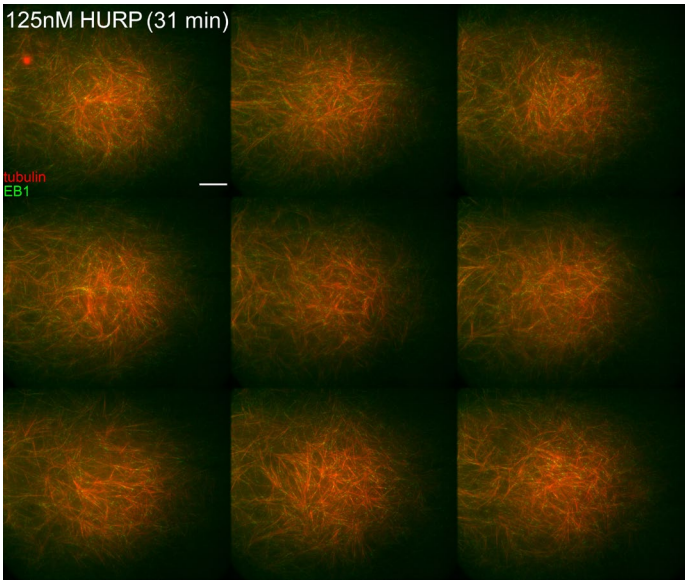

c

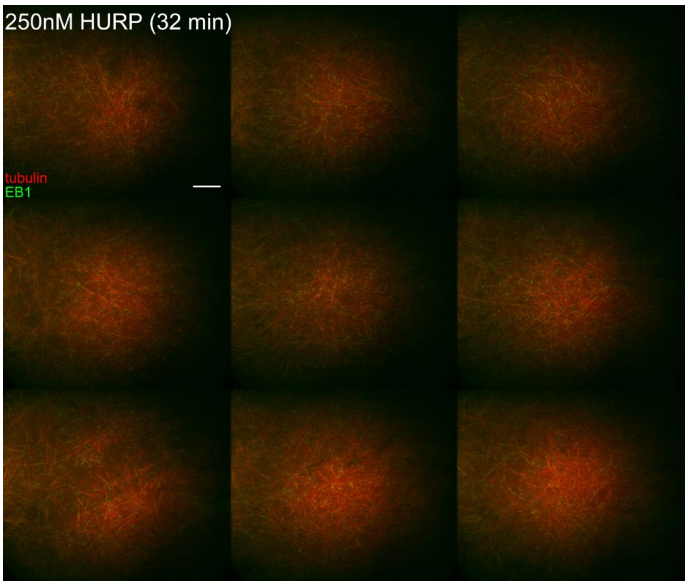

Supplementary Figure 5: Excess HURP induces formation of microtubules in *Xenopus* egg extract

3 x 3 images taken of the microtubule (MT) nucleation assays with varying concentrations of HURP after obtaining the movies displayed in Supplementary Movie 2. This was done to ensure that each movie obtained was representative of the reaction. **a** 3 x 3 image of the buffer condition after 34 minutes. **b** 3 x 3 image of the 125 nM HURP after 31 minutes. **c** 3 x 3 image of the 250 nM HURP condition after 32 minutes. MTs (Alexa647-tubulin) are pseudo-colored red and EB1-mCherry is pseudo-colored green for display purposes. Total field of view is 491.55 µm x 414.75 µm. Scale bars = 20 µm.

Supplementary Figure 6

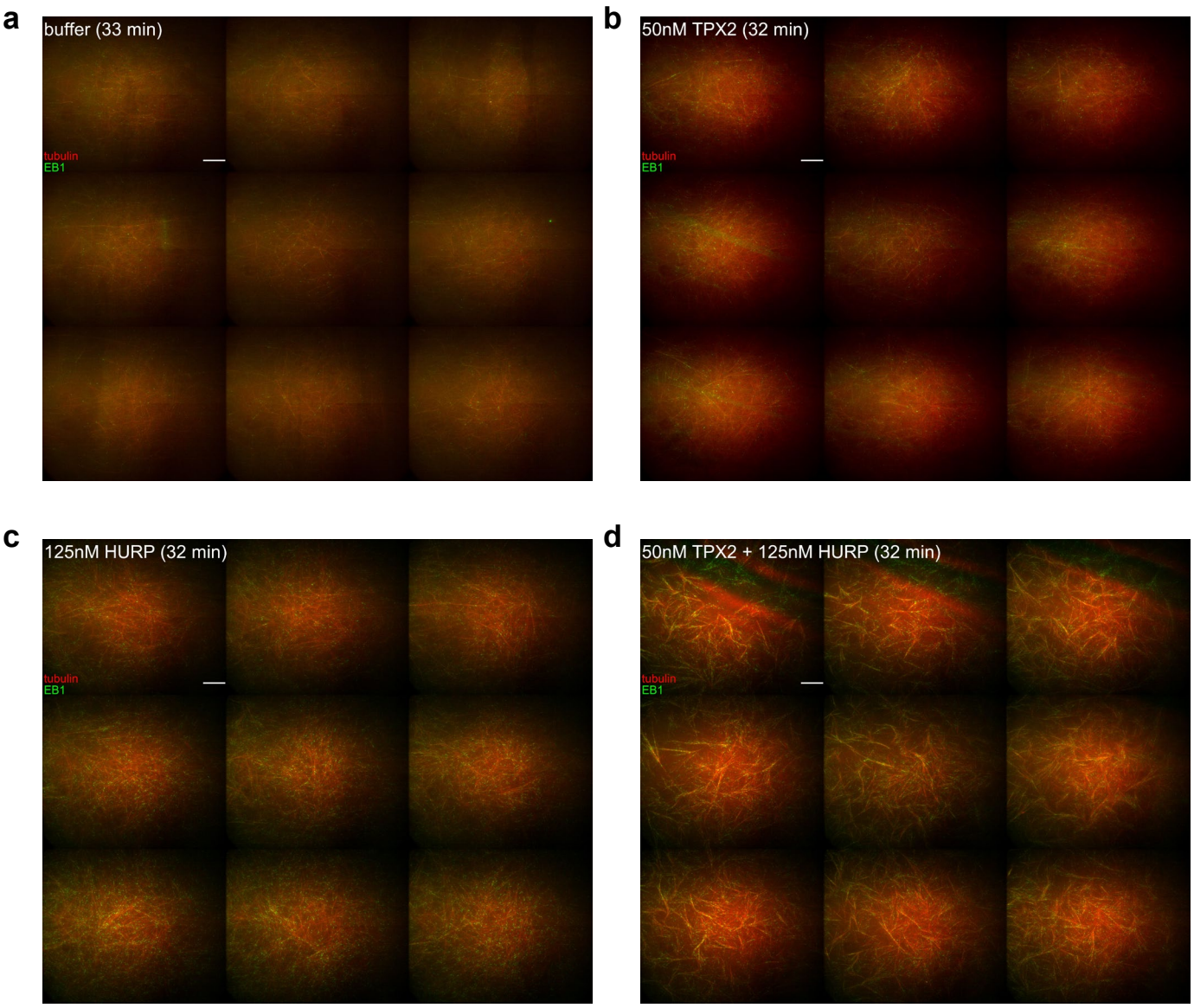

Supplementary Figure 6: TPX2 and HURP work together to form microtubules in *Xenopus* egg extract

3 x 3 images taken of the microtubule (MT) nucleation assays with HURP and TPX2 after obtaining the movies displayed in Supplementary 2. This was done to ensure that each movie obtained was representative of the reaction. **a** 3 x 3 image of the buffer condition after 33 minutes. **b** 3 x 3 image of the 50 nM HURP after 32 minutes. **c** 3 x 3 image of the 125 nM HURP condition after 32 minutes. **d** 3 x 3 image of the 50 nM TPX2 + 125 nM HURP condition after 32 minutes. MTs (Alexa647-tubulin) are pseudo-colored red and EB1-mCherry is pseudo-colored green for display purposes. Total field of view is 491.55 µm x 414.75 µm. Scale bars = 20 µm.

Supplementary Figure 7

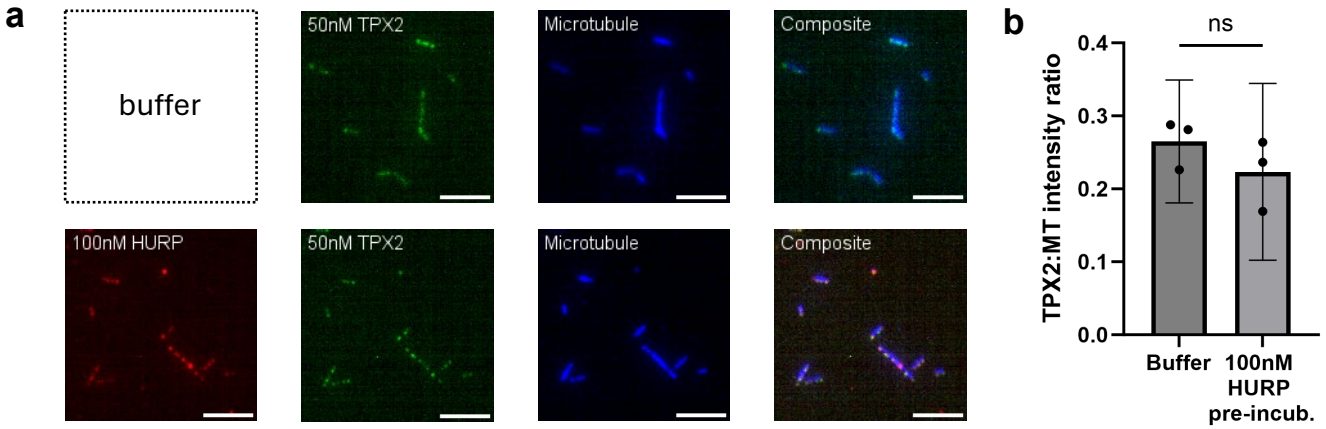

Supplementary Figure 7: HURP does not enrich TPX2 to the microtubule lattice

Sequential in vitro microtubule (MT) binding reactions using biotinylated, GMPCPP-stabilized MTs (ATTO647N-tubulin, pseudo-colored blue) bound to functionalized coverslips. **a** MTs were pre-incubated with 100 nM mCherry-HURP (n=3) or CSF-XB buffer (negative control, n=3), washed, then bound with 50 nM GFP-TPX2. MTs and bound proteins were imaged after a final BRB80 wash. Representative cropped images (39.77 µm x 39.77 µm) are displayed. Scale bars = 5 µm. **b** Bar graph plotting the average TPX2:MT intensity ratio across replicates (n=3) for each reaction in panel a. Individual points represent a single replicate (>25 MTs per replicate). Error bars represent the 95% confidence interval. P value = . Significance is defined as a p value < 0.05 by Welch's two-tailed t-test. ns = not significant

Supplementary Figure 8

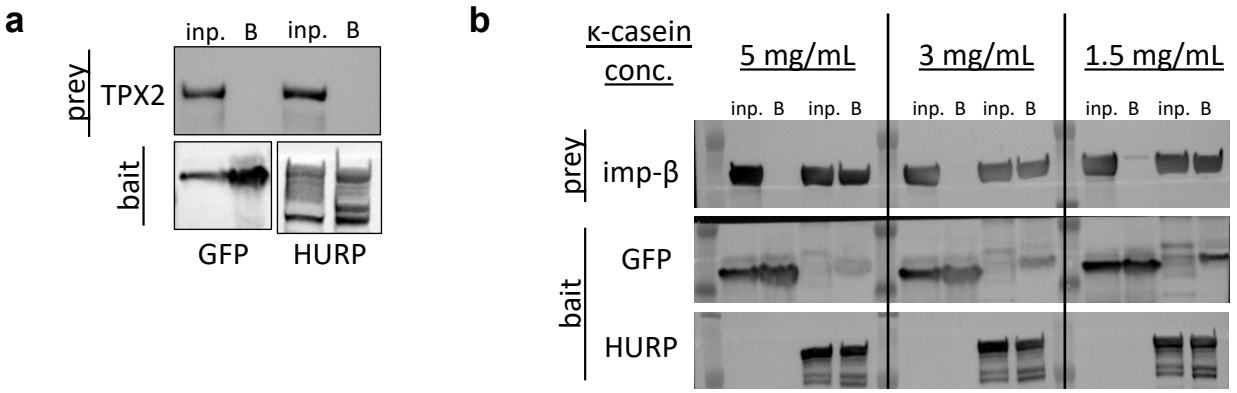

Supplementary Figure 8: HURP does not directly interact with TPX2 in solution

a Representative western blot of in vitro pull-down assay using 2 μM of GFP-HURP or His-GFP (negative control) as the bait and 2 μM GST-TPX2 as the prey. Baits were pulled down with GFP-Trap beads (ChromoTek). Input lanes (8% input) are denoted with "inp." and lanes for the bound fraction are denoted with "B". Repeated a total of three times with similar results. **b** Optimization of pull-down buffer condition (κ-casein concentration) using HURP's known interaction with importin-β as a positive control[3]. 2 μM of GFP-HURP or His-GFP (negative control) was used as the bait and 2 μM of GST-importin-β was used as the prey. Input lanes (8% input) are denoted with "inp." and lanes for the bound fraction are denoted with "B". 5 mg/mL κ-casein concentration was used for all pull-downs in this study. Uncropped blots are available in the source data file.

Supplementary Figure 9

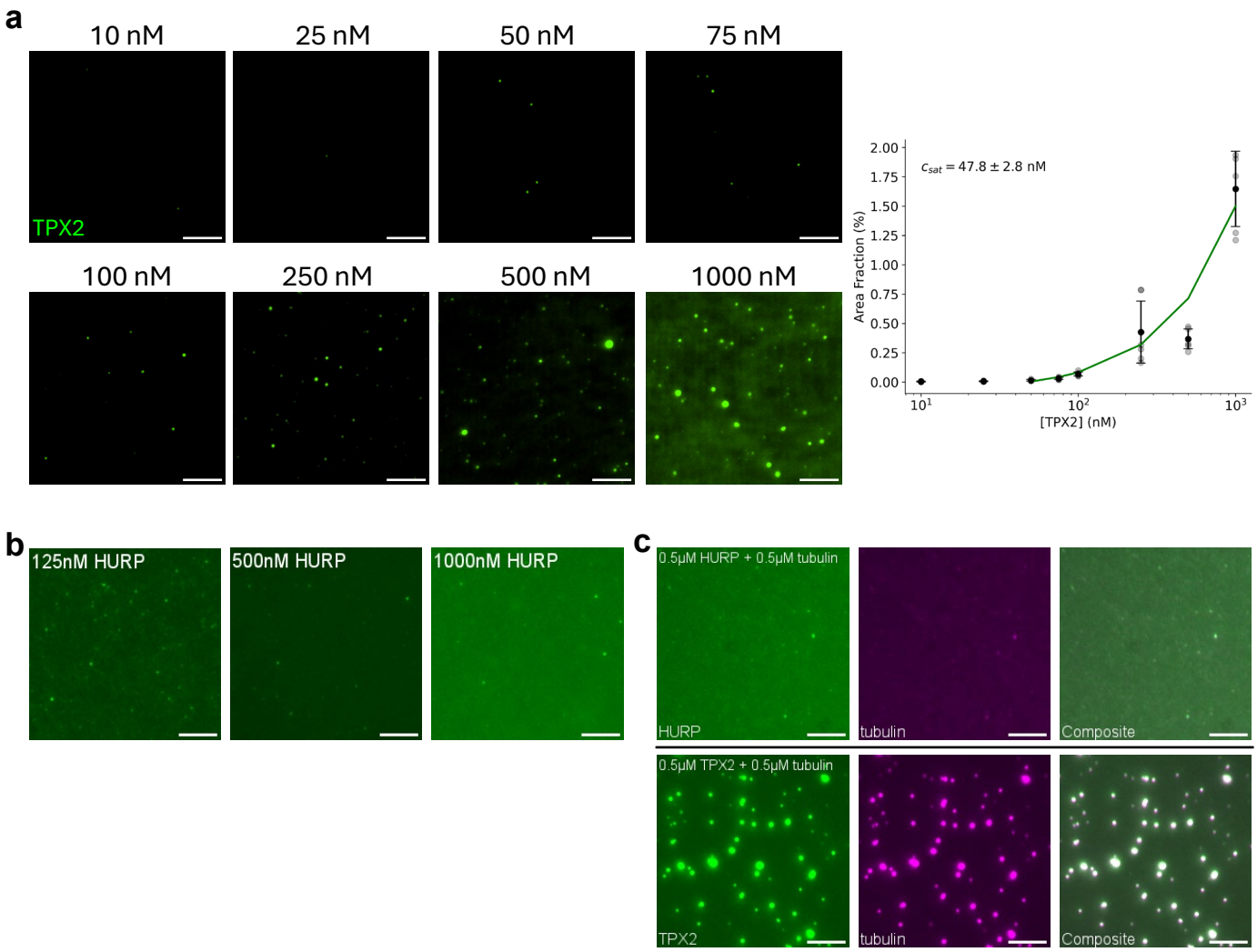

Supplementary Figure 9: HURP alone does not form phase condensates in vitro.

a Bulk phase assay in BRB80 buffer with increasing concentrations of purified GFP-TPX2. Determination of the phase boundary (nM ± standard deviation) by fitting a line to the mean area fraction (%) at each TPX2 concentration. Experimental repeats for each TPX2 concentration are as follows: for 10, 25, 50, 75, 100, and 25 nM (n = 3), for 500 and 1000 nM (n = 3). Each measurement (including technical repeats) are represented as a point on the plot. Error bars represent standard deviation. **b** Bulk phase assay in BRB80 buffer with increasing concentrations of purified GFP-HURP. **c** Bulk co-condensation assay in BRB80 buffer with equimolar Cy5-tubulin and GFP-HURP at 500 nM and 1 μM (top row). As a positive control, the same experiment was done with GFP-TPX2 (bottom row). Different conditions are separated by a black line. All images were taken at the surface of the coverslip to better visualize phase droplets. Representative cropped images (15.05 μm x 15.05 μm) are displayed. Scale bars = 5 μm.

Supplementary Figure 10

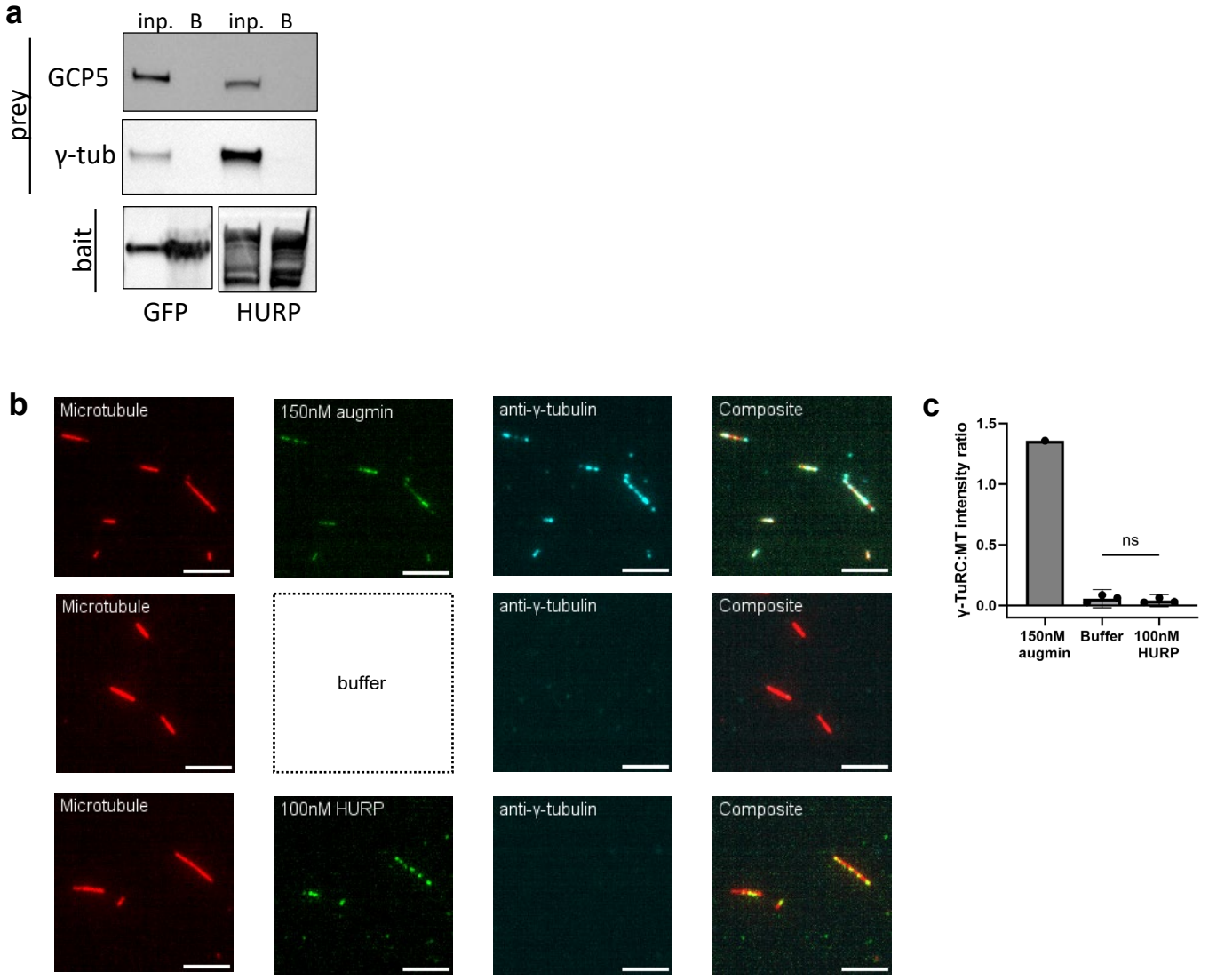

Supplementary Figure 10: HURP does not directly bind or recruit γ-TuRC to pre-existing microtubules

a Representative western blot of in vitro pull-down assay using 2 μM of GFP-HURP or His-GFP (negative control) as the bait and 40 nM γ-TuRC as the prey. Baits were pulled down with GFP-Trap beads (ChromoTek). Input lanes (8% input) are denoted with "inp." and lanes for the bound fraction are denoted with "B". Repeated a total of three times with similar results. Uncropped blots are available in the source data file. **b** In vitro microtubule (MT) binding reactions using biotinylated, GMPCPP-stabilized MTs (Alexa Fluor 568-tubulin) bound to functionalized coverslips. Each row of images portrays one experimental condition. MTs were incubated with a mix of 70 nM γ-TuRC and either 150 nM GFP-augmin (positive control, n=1), CSF-XB buffer (negative control, n=3), or 100 nM GFP-HURP (n=3) in CSFXB buffer. Alexa Fluor 647-conjugated γ-tubulin antibody was used to visualize γ-TuRC (pseudo-colored cyan). MTs and bound proteins were imaged after a final BRB80 wash. Representative cropped images (19.33 μm x 19.33 μm) displayed. Scale bar = 5 μm. **c** Bar graph plotting average γ-TuRC(γ-tubulin):MT intensity ratio. Individual points represent replicates (>25 MTs per replicate). Significance is defined as a p value < 0.05 by Welch's two-tailed t-test. ns = not significant.

Supplementary Figure 11

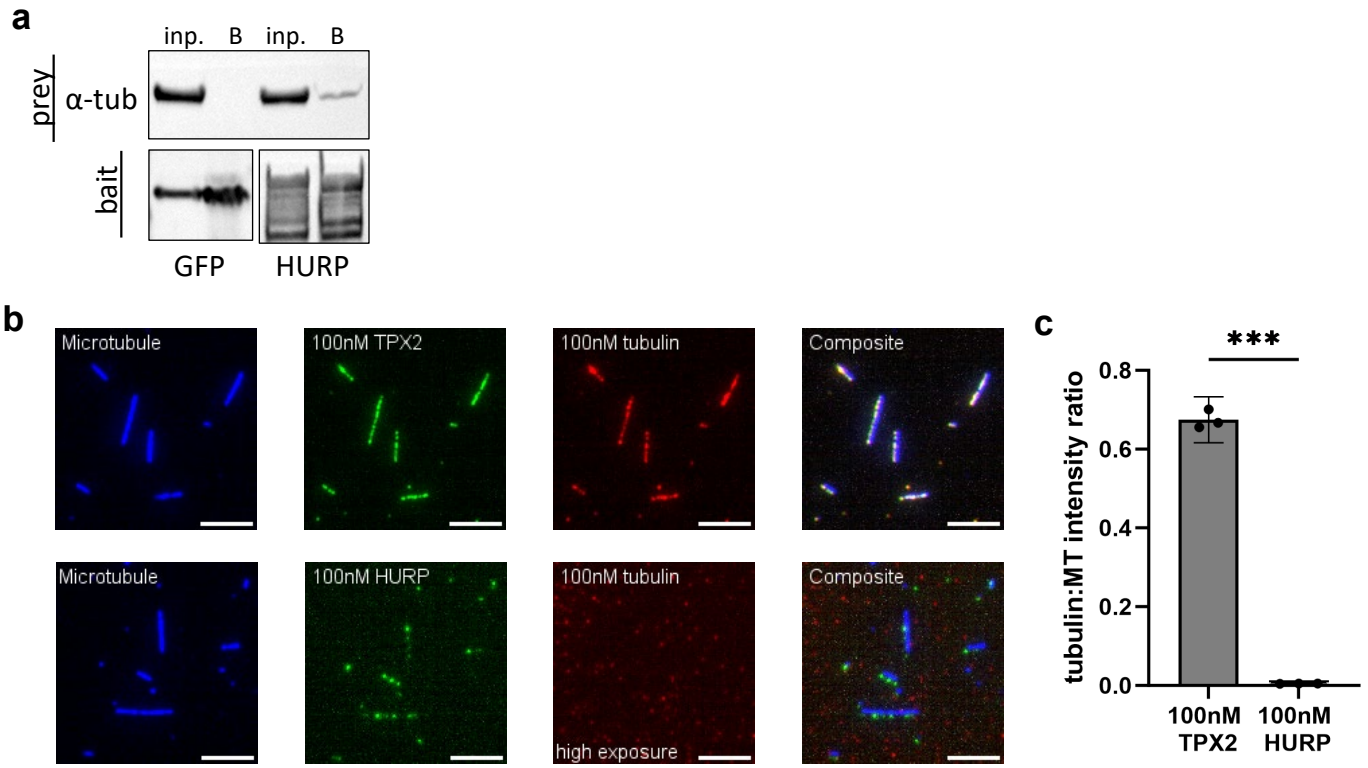

Supplementary Figure 11: HURP weakly binds to soluble tubulin but does not localize soluble tubulin to pre-existing microtubules.

a Representative western blot of in vitro pull-down assay using 2 μM GFP-HURP or His-GFP (negative control) as the bait and 2 μM soluble tubulin as the prey. The reaction was kept at 4°C to ensure no microtubule polymers were present. Baits were pulled down with GFP-Trap beads (ChromoTek). Input lanes (8% input) are denoted with "inp." and lanes for the bound fraction are denoted with "B". Repeated a total of three times with similar results. Uncropped blots are available in the source data file. **b** In vitro microtubule (MT) binding reactions using GMPCPP-stabilized and biotinylated MTs bound to coverslips. 100 nM soluble tubulin (Alexa Fluor 568-tubulin) was preincubated with either 100 nM GFP-TPX2 (positive control, n=3) or 100 nM GFP-HURP (n=3) prior to incubating with MTs. Each row of images represents a different reaction. Before imaging, MTs were washed with BRB80 buffer to remove unbound proteins. The tubulin channel for the HURP condition was taken at 25x higher exposure than the TPX2 condition to ensure visualization of any tubulin localization. Representative cropped images (39.77 μm x 39.77 μm) are displayed. MTs (ATTO647N-tubulin) were pseudo-colored blue for display. Representative Scale bar = 5 μm. **c** Bar graph plotting the average tubulin:MT intensity ratio for each MT binding reaction of panel a. For the HURP condition, the tubulin:MT intensity ratio was scaled down by a factor of 25 to account for the exposure difference to the TPX2 condition. Each individual point on the bar graph represents the average intensity ratio for each replicate. For each replicate, 30 or more MTs were measured. Error bars represent the 95% confidence interval. Significance is defined as a p value < 0.05 by Welch's two-tailed t-test. Triple asterisks (***) indicates a p value < 0.001.

Supplementary Figure 12

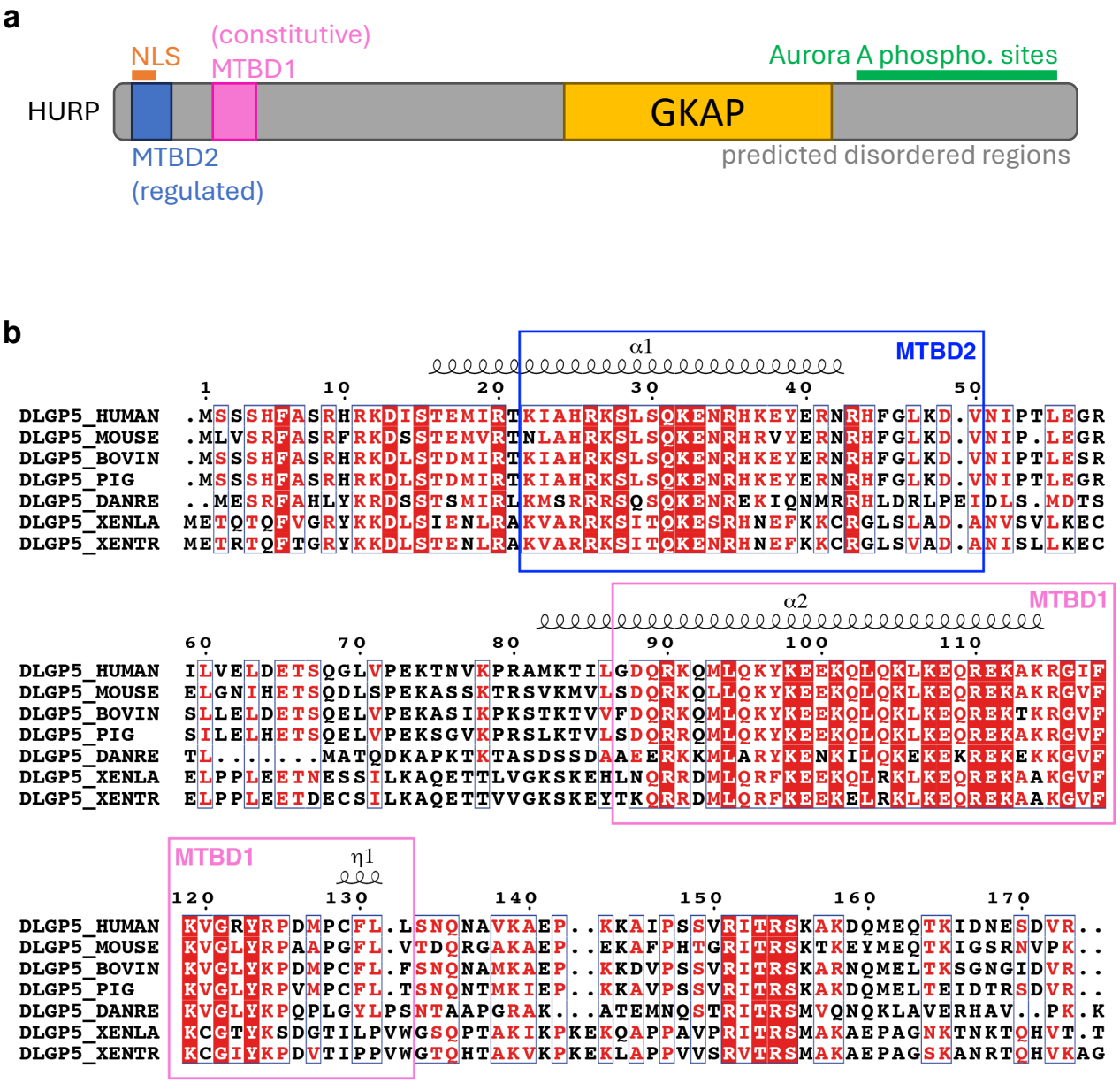

Supplementary Figure 12: Sequence alignment of HURP.

a Graphical schematic of the identified domains and putative binding sites of the human HURP protein. The microtubule binding domain 2 (MTBD2) is proposed to be regulated by importin-β binding at the nuclear localization signal (NLS)[4]. The microtubule binding domain 1 (MTBD1) is proposed to constitutively bind microtubules[5]. Guanylate kinase-associated protein domain (GKAP) with no known microtubule function. C-terminal region of Aurora A phosphorylation sites regulating microtubule binding and protein interactions[6,7]. Predicted disordered regions from the Alphafold2 prediction (grey). **b** The figure was prepared using ESPript 3.0[8] based on alignment results from Clustal Omega[9]. Human HURP sequence (DLGP5_HUMAN) was aligned to that of mouse, bovine, porcine (PIG), zebrafish (DANRE), *Xenopus laevis* (XENLA), and *Xenopus tropicalis* (XENTR). Secondary structure elements of HURP from Alphafold2 prediction (Figure 5) are shown above the sequences.

Supplementary Figure 13

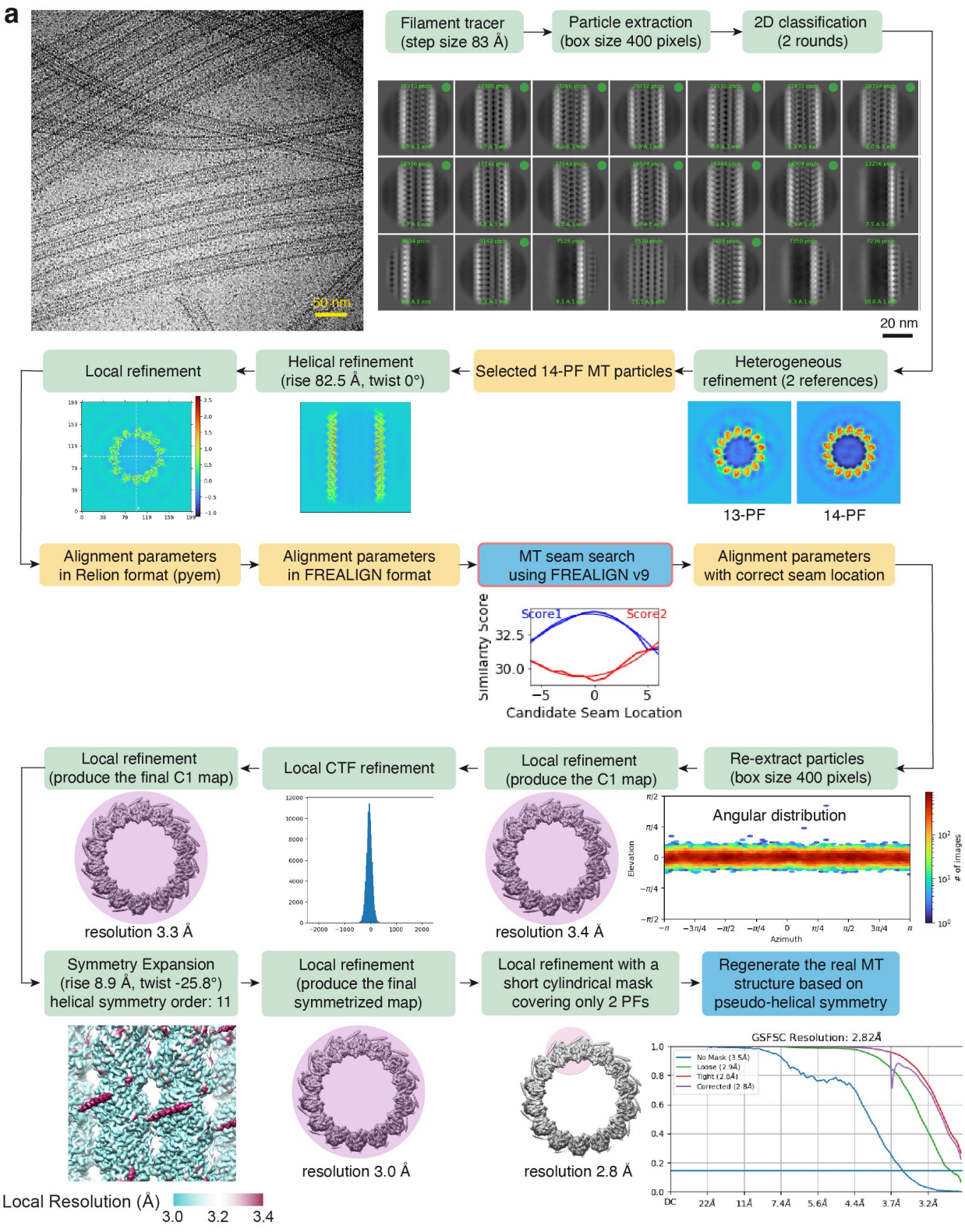

Supplementary Figure 13: Cryo-EM data processing of HURP-decorated microtubule

a Cryo-EM data processing scheme of HURP decorated microtubule. The local resolution was calculated with CryoSPARC v.4.6.

Supplementary Figure 14

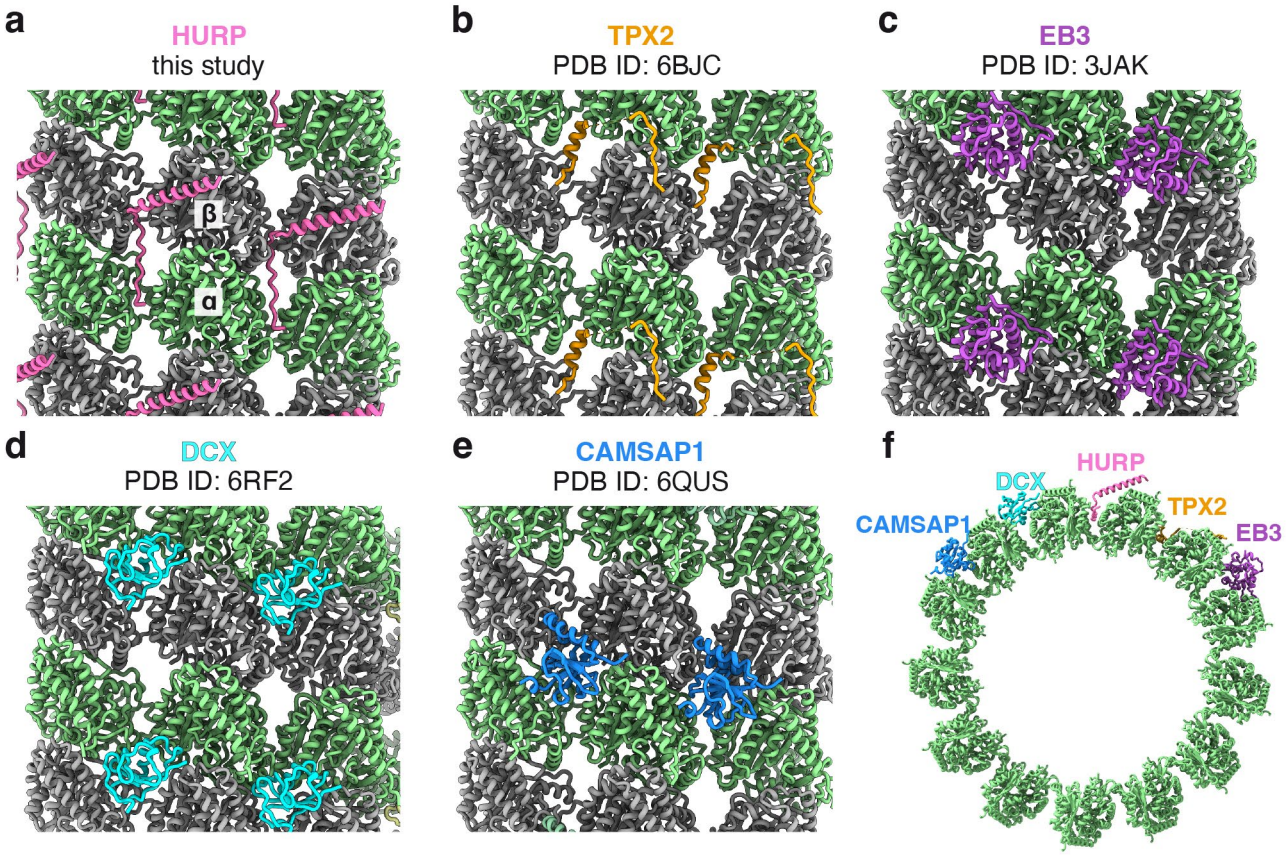

Supplementary Figure 14: Structural comparison of microtubule-associated proteins.

a-e Cryo-EM structures of HURP, TPX2, EB3, DCX and CAMSAP1 bound on microtubule **f** Hypothetical overlay of different MAPs on the same microtubule lattice.

Supplementary Table 1: Cryo-EM data collection, refinement, and validation statistics

	EMD-47173, PDB: 9DUQ
Data collection and processing	
Microscope	Titan Krios G3 (Thermo Fisher)
Detector	K2 Summit (Gatan)
Voltage (keV)	300
Nominal magnification	81,000×
Electron exposure ($e^-/Å^2$)	39.6
Defocus range set during data acquisition (mm)	-1.0 to -2.5
Pixel size (Å)	1.39
Symmetry imposed	C1
Initial particle no. (8 nm)	348,514
Final particle no. (8 nm, symmetry expanded)	2,936,725
Map resolution (Å)	2.8
Model composition	
Chains	45
Residues	8,127
Ligands	9 GTP / 9 G2P / 18 Mg
Refinement	
Resolution limit set in refinement (Å)	2.9
Correlation coefficient (CCmask)	0.8645
Root-mean-square deviation (bond lengths) (Å)	0.004
Root-mean-square deviation (bond angles) (Å)	0.636
Validation	
MolProbity Score	1.71
Clash score	10.52
Rotamer Outliers (%)	0.03
Ramachandran (favored) (%)	97.06
Ramachandran (outliers) (%)	0.00

Supplementary References

1. Searle, B. C. Scaffold: A bioinformatic tool for validating MS/MS-based proteomic studies. Proteomics 10, 1265–1269 (2010).
2. Wühr, M. et al. Deep Proteomics of the Xenopus laevis Egg using an mRNA-derived Reference Database. Current Biology 24, 1467 (2014).
3. Silljé, H. H. W., Nagel, S., Körner, R. & Nigg, E. A. HURP Is a Ran-Importin β-Regulated Protein that Stabilizes Kinetochore Microtubules in the Vicinity of Chromosomes. Current Biology 16, 731–742 (2006).
4. Song, L. & Rape, M. Regulated Degradation of Spindle Assembly Factors by the Anaphase-Promoting Complex. Mol Cell 38, 369–382 (2010).
5. Song, L., Craney, A. & Rape, M. Microtubule-Dependent Regulation of Mitotic Protein Degradation. Mol Cell 53, 179–192 (2014).
6. Didaskalou, S. et al. HURP localization in metaphase is the result of a multi-step process requiring its phosphorylation at Ser627 residue. Front Cell Dev Biol 11, (2023).
7. Wong, J., Lerrigo, R., Jang, C. Y. & Fang, G. Aurora A regulates the activity of HURP by controlling the accessibility of its microtubule-binding domain. Mol Biol Cell 19, 2083–2091 (2008).
8. Robert, X. & Gouet, P. Deciphering key features in protein structures with the new ENDscript server. Nucleic Acids Res 42, W320–W324 (2014).
9. Sievers, F. et al. Fast, scalable generation of high-quality protein multiple sequence alignments using Clustal Omega. Mol Syst Biol 7, 539 (2011).